Swelling Monitorization of Poly[(*N*-isopropylacrylamide)-*co*-(methacrylic acid)] Copolymers by Magnetic Resonance Imaging

I. Quijada-Garrido,* A. Prior-Cabanillas, L. Garrido, and J. M. Barrales-Rienda

Departamento de Química-Física de Polímeros, Instituto de Ciencia y Tecnología de Polímeros, Consejo Superior de Investigaciones Científicas, c/. Juan de la Cierva, 3, E-28006 Madrid, Spain

Received May 6, 2005; Revised Manuscript Received June 21, 2005

ABSTRACT: The dynamic swelling behavior in phosphate buffer solution (PBS) (pH 7) of poly[(*N*-isopropylacrylamide)-*co*-(methacrylic acid)] P[(N-iPAAm)-*co*-(MAA)] hydrogels has been studied by using magnetic resonance imaging (MRI), which provides information at a local level. To determine the water uptake at a global level, a gravimetric technique was also employed. Photographs were taken providing valuable information on the hydrogel morphology at different stages of swelling. By combining the data from these three methods, the pattern of water uptake may be clearly elucidated. The gravimetric swelling curves and photographs were in agreement with the information obtained from MRI images acquired on central slices of the hydrogels. In contrast to the homopolymers, when the corresponding copolymers hydrogels were soaked under acidic conditions (pH 2), they exhibited characteristic sigmoidal swelling curves at pH 7. Furthermore, the hydrogel slabs adopt a peculiar morphology as it was photographically observed. In the MRI images two processes were distinguished, corresponding to a highly swollen external region in contrast to a rigid core which starts to swell after a lag time depending on sample composition.

Introduction

In recent years, poly[(*N*-isopropylacrylamide)-*co*-(methacrylic acid)], P[(N-iPAAm)-*co*-(MAA)], copolymers have been a matter of study due to their potential applications as temperature- and pH-sensitive materials.[1−11] For example, these copolymers have been used for controlled delivery of an antihypertensive drug such as diltiazem hydrochloride,[12,13] antithrombotic,[1,4] and thrombolitic agents,[1] as a novel separation carrier in fluorescence immunoassays,[5] or in a glucose-sensitivity polymeric composite membrane for modulated permeation of insulin.[14] Thus, poly(*N*-isopropylacrylamide), P(N-iPAAm), exhibits thermosensitivity at about 32 °C, which is its lower critical solution temperature (LCST).[15,16] Poly(methacrylic acid), P(MAA), has in its structural unit ionizable carboxylic groups, which swell or collapse in response to changes of pH. The copolymerization of both results in systems with different properties depending on composition and previous swelling history,[9−11] which potentially allow obtaining hydrogels for specific uses. Copolymers with a high N-iPAAm content are able to respond to temperature changes depending on pH, whereas the ionizable carboxyl group of the MAA moiety furnishes for the whole range of copolymer composition pH-sensitivity. Additionally, these copolymer hydrogels exhibit strong interactions among their comonomeric units.[8,9] By means of solid-state NMR, hydrogen bond arrangements between the carboxylic groups of methacrylic acid (MAA) and the amide groups of the N-iPAAm units have been detected.[8,17] Hydrogen bonding occurs at low pH below the pK_a of MAA comonomeric units, and it disrupts at neutral and high values of pH with a slowly swelling rate. An anomalous behavior has been found in the swelling experiments, which was explained by the reversible character of the hydrogen bonds when the pH of the medium is changed.[10,11] Copolymers soaked under acidic pH exhibited sigmoidal swelling curves under neutral and basic pH. The origin of this behavior has been attributed to the disruption of the hydrogen bond arrangements formed at acidic pH.

Sigmoidal swelling curves for water uptaking may be found in the literature for some other systems.[18−30] Thus, Siegel et al.[18,19,22] and Falamarzian et al.[23] found this anomalous behavior for hydrophobic weak base polyelectrolite copolymers of methyl methacrylate (MAA) and *N,N*-dimethylamino methacrylate (DMA), when they swell under acidic media. On the other hand, Okano and co-workers[20,21] found sigmoidal swelling curves for thermoresponsive hydrogels of poly[(N-iPAAm)-*co*-(*n*-butyl methacrylate)], a system with some different characteristics to that one studied by Siegel et al.[19] They reconcile their model with the Siegel's[19] so-called "swelling front model".

All these theories to explain the sigmoidal swelling curves and some others given by some of the present authors[10,11,31,32] have been established on the observation of the phenomena at a global level. For this reason, a study of the swelling by magnetic resonance imaging is quite interesting because it provides a spatial and a temporal resolution of the process.

Magnetic resonance imaging (MRI) is a noninvasive imaging technique which has found widespread application in hydrogels to monitor the change in water uptake with time, thus allowing the study of swelling in real time. MRI is sensitive to mobile protons of solvents and as such is particularly useful for studying their diffusion processes.[33−37] MRI has been used widely to monitor the diffusion of water and other solvents into synthetic polymers.[38] This capability can quite naturally be applied to polymer-based controlled release systems.[39−41]

The theory and experimental of the MRI technique have been described and reviewed.[42,43] This technique allows the collection of images of the system undergoing changes as a function of time from an unique specimen which obviates the inherent sample-to-sample differences. Thus, MRI would provide valuable information

* Corresponding author: Tel +34-91-562 29 00; Fax +34-91-5644853; e-mail iquijada@ictp.csic.es.

10.1021/ma0509513 CCC: $30.25
Published on Web 07/21/2005

about the anomalous swelling behavior of the P[(N-iPAAm)-*co*-(MAA)] copolymers. Because of the nondestructive character of MRI, the hydrogel hydration can be monitored to yield information on the spatial and temporal variation of distribution of water within the polymer. In other words, the polymers obtained were studied regarding their kinetic swelling ability. Also, we determined in detail the influence of copolymer composition on the swelling properties.

Experimental Section

Materials. The monomer *N*-isopropylacrylamide, (N-iPAAm) (113.16 g/mol) (Acros Organics, Fairlawn, NJ), 99% purity, was purified by recrystallization from a *n*-hexane/toluene mixture (90/10 vol %). Methacrylic acid (MAA) (86.09 g/mol) (Fluka Chemie A. G., Buchs, Switzerland), 98% purity, for synthesis and stabilized with 0.025% hydroquinone monomethyl ether and sodium dihydrogen phosphate anhydrous (purum ≥ 99.0%) for PBS solutions was used as received. The cross-linker tetraethylene glycol dimethyl acrylate (TEGDMA), stabilized with ≈0.006% hydroquinone, the activator *N,N,N′,N′*-tetramethylethylenediamine (TEMED), and the initiator ammonium persulfate (APS) both for molecular biology from (Fluka Chemie and Biochemie A. G., Buchs, Switzerland) were used as received. Ethanol reagent degree (Scharlau, Barcelona, Spain), disodium hydrogen phosphate anhydrous purisimum used for buffer solutions (phosphate buffer solutions, PBS), *n*-hexane, toluene, and sodium chloride for analysis and sodium hydroxide purum (Panreac Química S. A., Barcelona, Spain) were used as received. Water for all reactions, solution preparation, and hydrogels purification was Milli-Q from a water purification facility (Millipore Milli-U10). Gadopentetate dimeglumine, Gd-DTPA (Shering AG, Germany), was used to reduce the spin−lattice relaxation time, T_1, of water protons.

Synthesis. P(N-iPAAm), P[(N-iPAAm)-*co*-(MAA)], and P(MAA) gels were synthesized by free-radical cross-linking copolymerization in solution of the monomers N-iPAAm and MAA. Polymerization was carried out using a mixture of water and ethanol 60/40 v/v as solvent. Six different copolymers were obtained with N-iPAAm % molar composition of 100, 62, 42, 25, 13, and 0, as determined by elemental analysis by using a CHN EA 1108 elemental analyzer (Carlo Erba Instruments S. p. A., Milano, Italy). In all cases a ratio of monomers/solvent ratio of 1:1 (w/v) (14 g of monomers per 14 mL of a solvent mixture of water/methanol) was used. In some instances, for high content of MAA copolymers, MAA monomer was neutralized by means of an aqueous NaOH solution. Cross-linker TEGDMA, activator TEMED, and initiator APS were used with an initial weight ratio of 0.5 wt % of the total monomer amount (14 g).

The following procedure to obtain sheet shape gels was employed. The mixture solution was cast on glass plates (120 × 100 × 3 mm) enclosed by a rubber framework-spacer with 1 mm thickness and sealed off with other glass plate in order to avoid air contact during polymerization. The gelation takes place within 3 h. Afterward, the gels were removed from the glass plate and immersed in freshwater for 3 days to remove the unreacted chemicals. During this time the water and chemicals dissolved were five times removed and replaced by fresh Milli-Q water. Uniform disks with a diameter of 15 mm and a thickness of 1 mm were punched out the gel sheet using a stainless steel cork borer. These disks were left to dry at room temperature for 24 h and then vacuum-dried (10^{-3} mmHg) at 60 °C for 12 h. Since the previous swelling history was shown to have a strong influence on the swelling behavior,[11] samples from synthesis were soaked under acidic medium (pH 2) for 48 h and dried in a vacuum oven at 60 °C for 24 h; with this treatment hydrogen bond arrangements are allowed.

Gravimetric Swelling. Dried presoaked under acidic medium disks were left to swell in PBS at pH 7 (ionic strength = 0.1 M) at 25 °C. After regular time intervals samples were taken out, wiped superficially with blotting paper, weighed, and placed again in the same bath. The swelling ratio or degree of swelling, Q_t, at a time t was calculated in grams of water per grams of dry gel (xerogel) using the following expression:

$$Q_t = (m_t - m_0)/m_0 = W_t/m_0 \quad (1)$$

where m_t is the weight of the swollen gel at time t, m_0 is the weight of the dried gel (xerogel), and W_t is the weight of the water uptake at time t. The normalized swelling rate is obtained by the next relation Q_t/Q_∞, where Q_∞ is the swelling at equilibrium.

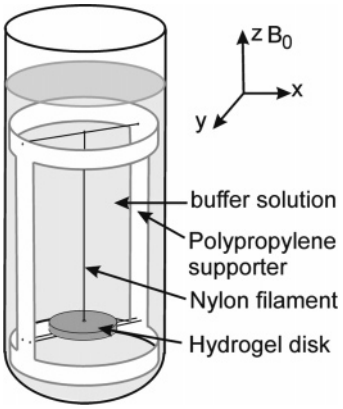

Figure 1. Size and position setup for the disk arrangement in the NMR imaging swelling experiment. Inside of a glass tube of 2 cm diameter with phosphate buffer, a disk hold to a PP supporter by several nylon filaments is placed. With this arrangement the shortest dimension of the disk is parallel to the magnetic field B_0.

Photographic Swelling Fronts. Photographs of the hydrogel disks were recorder with a Panasonic digital video camera Mini DV PAL (Matsushita Electric Industrial Co., Ltd., Osaka, Japan) at regular time intervals during the gravimetric experiment.

Magnetic Resonance Imaging (MRI). All proton NMR imaging experiments were carried out on a Bruker Avance 400 spectrometer/imager (Bruker Analytik GmbH, Karlsruhe, Germany) equipped with a Bruker UltraShield 9.4 T (^{1}H resonance frequency of 400.14 MHz), 8.9 cm vertical-bore superconducting magnet. The maximum strength of the magnetic field gradient is 97.3 G/cm. The NMR images were acquired at room temperature by using a standard Bruker imaging probe with a 25 mm diameter rf insert. A standard Bruker 2D spin echo pulse sequence was used to acquire the data which were converted into proton density maps using Paravision software supplied with the spectrometer. An echo time TE of 4.393 ms and a repetition time TR of 1 s were used. Four scans were averaged for each image with a field of view (FOV) of 30 × 30 mm and a slice thickness of 0.25 mm. For each image a non isotropic matrix of 256 × 128 pixels with a spatial resolution of 117 × 234 μm was acquired. To keep the sample at the same spatial position during the experiment, each hydrogel disk was supported on two nylon filaments and a third filament crossing its center. All three were fixed to a polypropylene supporter as shown in Figure 1.

Experimental Results

Macroscopic Swelling Experiments: Gravimetrical Technique and Photographs. Figure 2 shows dynamic gravimetric swelling curves at pH 7 of P(MAA) of a series of P[(N-iPAAm)-*co*-(MAA)] copolymers having 13, 25, 42, and 62 mol % of N-iPAAm content and P(N-iPAAM). All these hydrogels were previously soaked at pH 2. In general, it could be said that the behavior of the copolymer hydrogels is different compared to those of their corresponding P(MAA) and P(N-iPAAM) homopolymers. As a first insight, both swelling rate and curve shape strongly depend on composition. Swelling curves

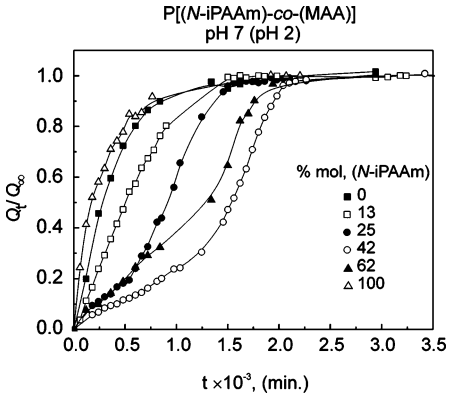

Figure 2. Normalized gravimetric swelling isotherms in water at pH 7 and 25 °C previously soaked at pH 2 of a series of samples of P(MAA), 13, 25, 42, and 62% mol N-iPAAm copolymers and P(N-iPAAm) cross-linked with 0.5 wt % of TEGDMA.

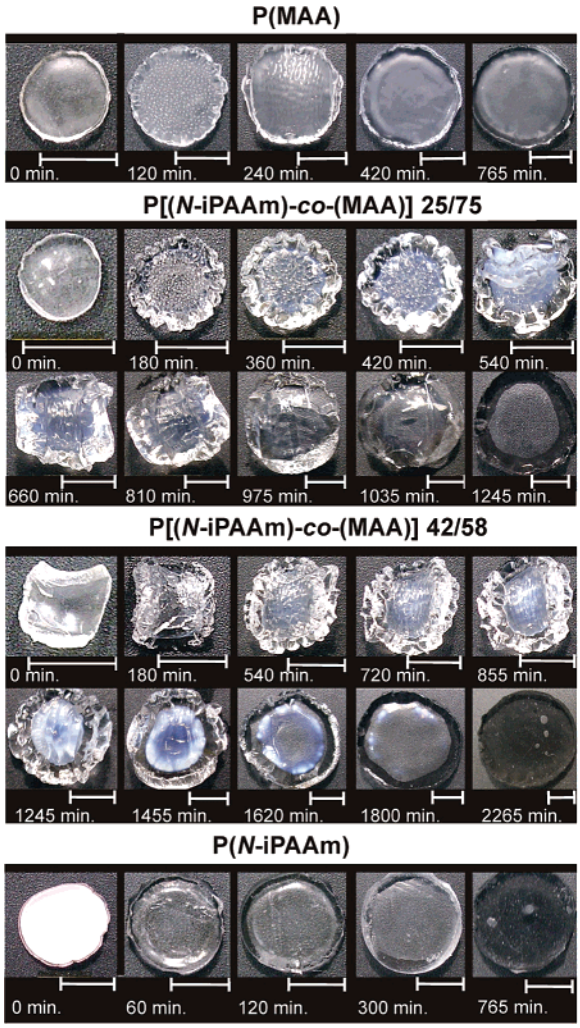

Figure 3. Time-dependent photographs taken at different stages of swelling of disk-shaped P(MAA), two P[(N-iPAAm)-*co*-(MAA)] copolymers having 25 and 42% mol of N-iPAAm content, and P(N-iPAAm) at pH 7 and 25 °C and previously soaked at pH 2. The scale bar represents 0.5 cm.

corresponding to the copolymers exhibit a typical sigmoidal shape.

In Figure 3, time-dependent photographs of disk samples of P(MAA) and P[(N-iPAAm)-*co*-(MAA)] copolymers with 25 and 42% mol N-iPAAm and P(N-iPAAm) taken at different stages of swelling are shown. It is

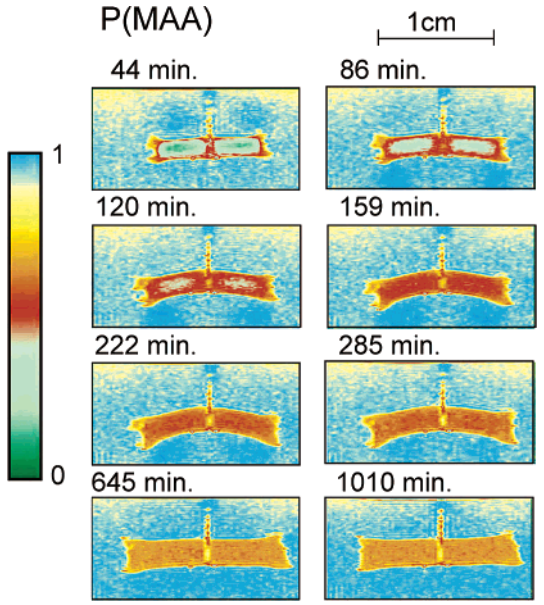

Figure 4. Proton MRI images corresponding to the dynamic swelling isotherms of P(MAA) cross-linked with 0.5 wt % of TEGDMA in water at pH 7 and 25 °C and previously soaked at pH 2.

observed that the morphology of the copolymer hydrogels during swelling differs clearly from that of their corresponding homopolymers. It seems that the diameters of P(MAA) and P(N-iPAAm) disks increase progressively until the equilibrium is reached. However the disks copolymers prepared display a scalloped pattern on the surface and edges. This behavior has been observed also in the case of P[(N-iPAAm)-*co*-(BMA)] by Yoshida et al.[20] They attributed the pattern observed to an anisotropic swelling of the samples, and our MRI results are in agreement with this interpretation. Simultaneously when this pattern is developed, a white-opaque core may be observed which persists during a long time, thus 750 min for the copolymer with 25% mol N-iPAAm and 1800 min for the copolymer with 42% mol N-iPAAm, approximately.

Swelling Monitorization by Magnetic Resonance Imaging (MRI). Figures 4, 5, and 6 show ^{1}H NMR images corresponding to different stages of swelling for hydrogels with 0, 25, and 100% mol N-iPAAm content. Color maps represent the relative proton signal intensity. The most mobile region, corresponding to the water outside the gel, gives the highest intensity and it can be seen in blue. Rigid regions from the nonhydrated gel are seen in dark green. For the whole series of hydrogels, the swelling front may be seen in yellow. P(N-iPAAm), as it was observed in the gravimetric experiment, exhibits the fastest swelling rate (Figure 6); in the first image recorded after 13 min, water had already penetrated reaching the sample center (the dark green region could not be observed). P(MAA) presented a slower swelling rate (Figure 4) than P(N-iPAAm), but also a more rapid swelling than copolymers, at relative early stages (about 44 min) water was able to reach the sample core, after 159 min; as it can be seen the whole sample is uniformly hydrated, later on, water uptaking continues monotonically until equilibrium is reached. A comparison between the swelling behavior of the homopolymers and copolymers reveals clear differences. The swelling of the homopolymers occurs uniformly, whereas copolymers exhibit two swelling regions, an outer part swollen extensively and an inner one or core

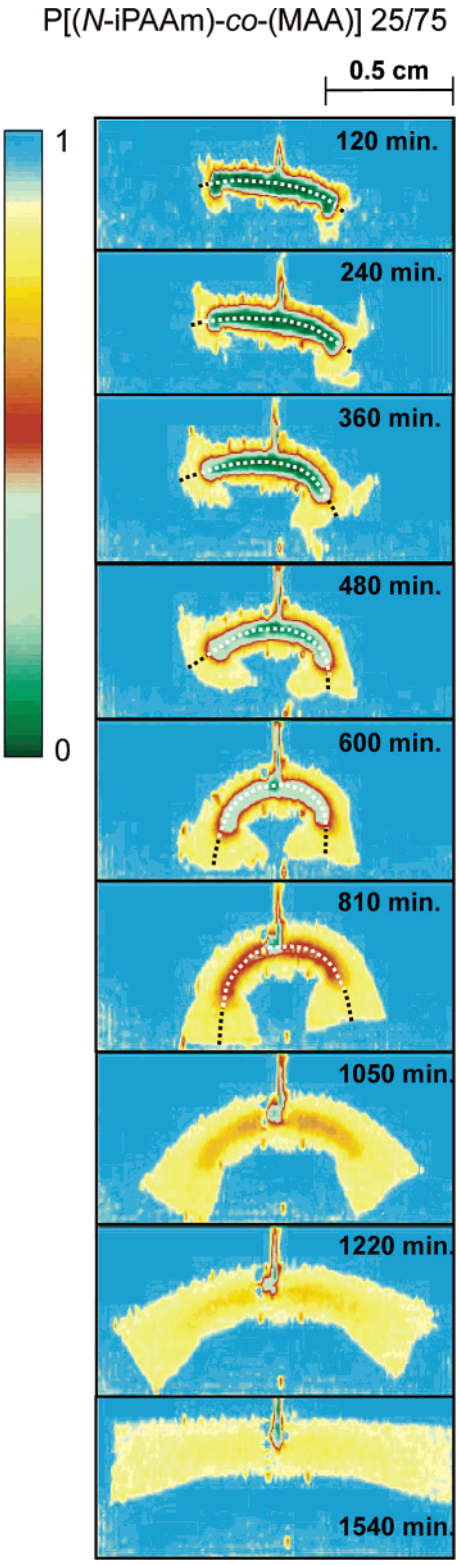

Figure 5. Proton MRI images corresponding to the dynamic swelling isotherms of P[(N-iPAAm)-*co*-(MAA)] 25/75 cross-linked with 0.5 wt % of TEGDMA in water at pH 7 and 25 °C and previously soaked at pH 2. The dotted white and black lines represent the two swelling processes.

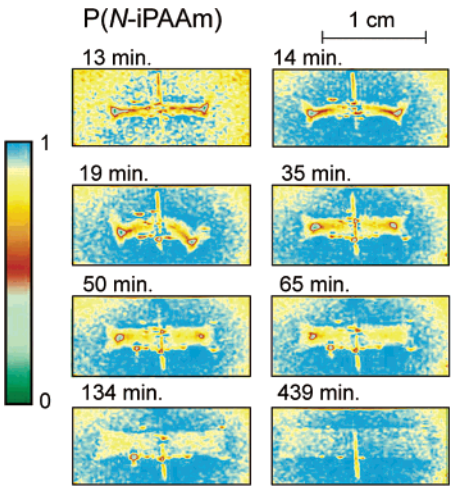

Figure 6. Proton MRI images corresponding to the dynamic swelling isotherms of P(N-iPAAm) cross-linked with 0.5 wt % of TEGDMA in water at pH 7 and 25 °C and previously soaked at pH 2.

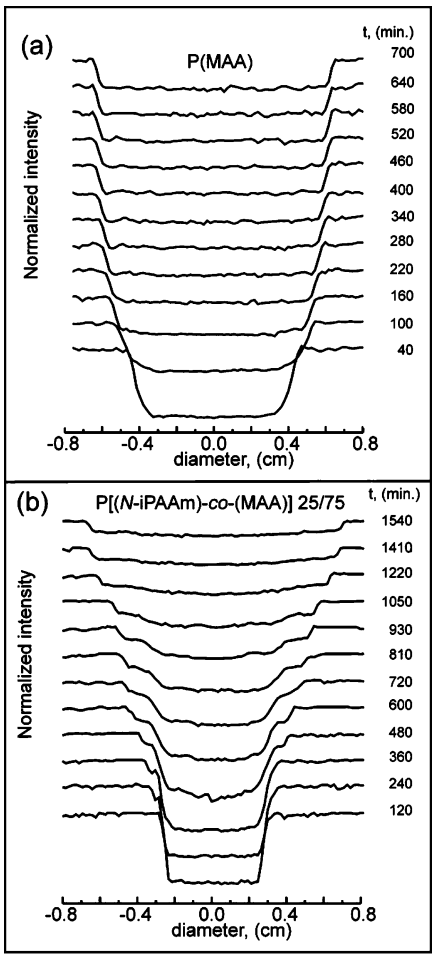

Figure 7. One-dimensional signal intensity profiles obtained from (a) P(MAA) and (b) P[(N-iPAAM)-*co*-(MAA)] 25/75, after varying time of swelling as it is indicated. A part of the primary data are given in Figures 4 and 5. The profiles correlate quite well with the phases and interfaces taken for the same hydrogels photographically as it is explained in the text.

nonhydrated. Comparing the swelling process of all copolymers (images not shown), it can be appreciated that the slowest swelling occurs for the hydrogel with a N-iPAAm content of 42% mol. For this sample, the nonhydrated region at the sample core can be observed for more than 1 day (~2000 min). This hard core corresponds to the white-opaque region observed in the photographs. Figure 7 illustrates one-dimensional signal intensity profiles obtained from images, at increasing swelling time, corresponding to samples of P(MAA) (a) and the copolymer with 25% mol N-iPAAm (b). The difference in the swelling behavior of these two hydro-

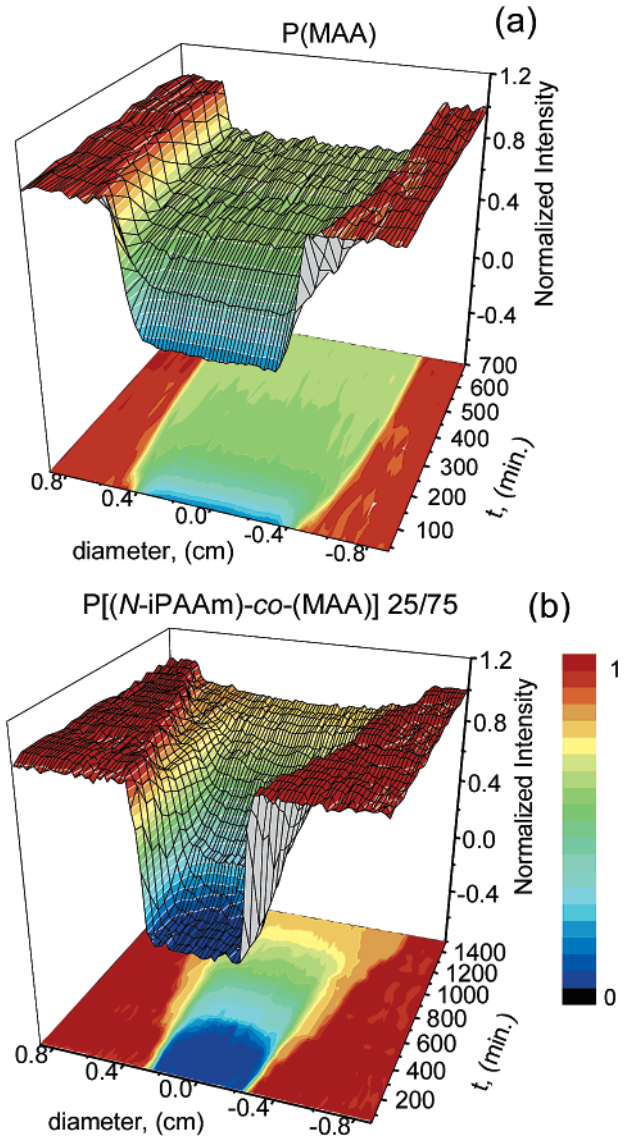

Figure 8. Three-dimensional surfaces representing the spin density profiles as a function of the swelling time: (a) P(MAA) hydrogel polymer; (b) P[(N-iPAAm)-*co*-(MAA)] 25/75.

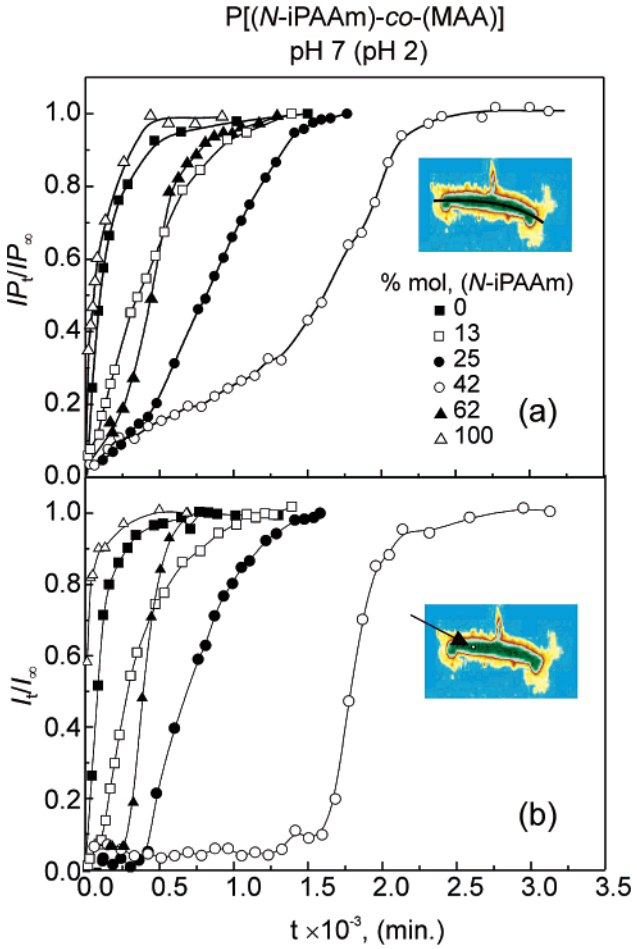

Figure 9. Swelling curves obtained from MRI images of a series of samples of [P(MAA)] and P[(N-iPAAm)-*co*-(MAA)] copolymers and [P(N-iPAAm)], all cross-linked with 0.5 wt % of TEGDMA in water at pH 7 and 25 °C and previously soaked at pH 2: (a) as a function of the normalized integral of the spin density profiles IP_t/IP_∞ vs time t, measured along the concave axis of the sample; (b) as a function of the normalized intensities, I_t/I_∞, measured at a point as it is indicated in this figure.

gels can be seen easily. The P(MAA) homopolymer shows a progressive and homogeneous swelling since the first stages, whereas the copolymer presents a more complex behavior, namely the presence of the two overlapped processes, as we already suggested by means of a gravimetric analysis.[11] First of all, we may observe the appearance of two well-differentiated zones, as mentioned above, i.e., an external zone, with swelling values closed to the equilibrium. It moves very slowly, appearing in the photography as the refolded border, and an internal zone which remains unchanged up to the acceleration process has been initiated. This fact is shown in a very illustrative form in the three-dimensional and contour map plots which are shown in Figure 8. Here, it is shown a fast and uniform swelling taking place in the homopolymer P(MAA); on the contrary, in the copolymer, we can observe that the internal zone in blue is not accessible to the water until ~400 min; at this moment the water starts to hydrate this zone, thus producing the acceleration in the swelling. It is worthwhile to point out that once this second process has started, the swelling in the inner zone takes place in a quite homogeneous fashion. It does not exist practically an intensity gradient along this zone. As long as this second process does not take place, the water swells the external zone of the gel, reaching then the values which are attained when the sample is completely swollen (yellow zone).

At this point, we must paid especial attention to the photographs displayed in Figure 3, on which we have made before some comments. As we can see, for the copolymers, there is a very peculiar wide edge, which may be due to the folding of the most external zone. It is highly swollen as it has seen by means of the MRI images.

From the integral of the MRI signal intensity profiles at each time, IP_t, a curve can be estimated which is related to the swelling process. The normalized integral intensity, IP_t/IP_∞, where IP_∞ is the integral of the intensity profile when equilibrium is attained, for each one of the samples is plotted in Figure 9a. The trend of these curves is very similar to that one obtained from the gravimetric experiment (Figure 2); however, swelling seems to be faster for the NMR imaging experiment. This fact could be due to the effect of the hole at the sample center. Nevertheless, the sigmoidal shape, occurring for some of the hydrogels, is reproduced quite well in the NMR imaging experiment.

In Figure 9b the evolution of the signal intensity at a middle point, namely in between the center of the sample and its edges is plotted. At this point we can see clearly the existence of a delay time in the copolymers; after this time the swelling occurs in almost an exponential fashion.

Analysis of the Swelling Kinetics. From the classical point of view of molecular dynamics, the swelling process has been classified in the recent past according to the following criteria: diffusion in polymers takes place by the transport of a penetrant via random molecular motion.[44] (i) Case I or Fickian, in which the rate of diffusion of the penetrant is much less than that of polymer segment mobility. (ii) Case II, in which the rate of diffusion is much greater than polymer segment mobility and is strongly dependent on swelling kinetics. (iii) Anomalous or non-Fickian in which rate of diffusion is comparable with polymer segment mobility. Cases I and II represent two extremes of diffusion behavior, with anomalous diffusion falling in between.[45]

These three general cases are related to the exponent n of the following heuristic equation:[46,47]

$$M_t/M_\infty = kt^n \tag{2}$$

where M_t is the water uptake, M_∞ is its final value (equilibrium value), k is a constant characteristic of the system, n is an exponent characteristic of the penetrant transport mechanism, and t denotes time. For a film, $n = 0.5$ indicates Fickian kinetics, $n > 0.5$ indicates non-Fickian or anomalous transport, and $n = 1$ implies case II (relaxation-controlled) transport.

However, Siegel[19] indicated that in the case of ionizable gels, in addition to solvent diffusion and polymer relaxation, ion diffusion and fixed charge groups ionization rates have to be taken into account.

For many years the cases of anomalous diffusion have been attributed to relaxation phenomena in the polymer; thus, for instance, Berens and Hopfenberg[48] described this process by means of a first-order kinetics:

$$M_t/M_\infty = 1 - e^{k_R t} \tag{3}$$

However, neither eq 2 nor eq 3 seems to fit satisfactorily all the experimental results, especially in those cases where sigmoidal swelling curves are observed.

To describe quantitatively the water uptake in the homopolymers and copolymers synthesized, it is necessary to find an appropriate model. In a previous work, we have analyzed in detail the swelling kinetics of this type of copolymer, as a function of pH, composition, and temperature and also by taking into account the swelling history of the samples (by controlling the soaking pH).[10,11,31,32] We found that swelling may be accurately described by means of a first-order kinetics when hydrogels are free of hydrogen bond arrangements, i.e., samples soaked at pH 7 and subsequently soaked again at the same pH.[32] However, we did not found a kinetics model in the literature which could describe the swelling for the observed sigmoidal curves in the copolymers at pH 7 when they were previously soaked in acidic medium. Sigmoidal curves were related to the dynamic disruption of hydrogen-bonding arrangements, formed previously at acidic pH between both comonomeric units, following an autocatalytic process.[11] The acceleration was justified according a cooperativity disruption of the hydrogen bonding and hydrophobic interactions when water penetrates inside the gel these interactions weakness and every time the penetration of new molecules of water take place easier.

The water uptake can be considered as follows:

$$H_2O \xrightarrow{k_1} H_2O^\bullet$$

$$H_2O + H_2O^\bullet \xrightarrow{k_2} 2H_2O^\bullet \tag{4}$$

where $H_2O^\bullet$ represents water molecules inside the gel; the first water molecule that penetrates inside the polymer helps to the next one to go inside the gel, so that $k_2 \gg k_1$. This is a water penetrating kinetics scheme for a simple autocatalytic process. In the present case, the swelling rate is proportional to the amount of sites still available for water, $1 - Q_t/Q_\infty$, and to the water already inside the gel, Q_t/Q_∞; therefore, we can write as

$$d(Q_t/Q_\infty)/dt = k_1[1 - (Q_t/Q_\infty)] + k_2 Q_t/Q_\infty[1 - (Q_t/Q_\infty)] \tag{5}$$

which after integration and arrangement yields the following equation:

$$\frac{Q_t}{Q_\infty} = \frac{(k_1/k_2)(1 - e^{-(k_1+k_2)t})}{(k_1/k_2) + e^{-(k_1+k_2)t}} \tag{6}$$

When $k_1 \gg k_2$, $k_1 + k_2 \approx k_1$, and therefore $k_1/k_2 \gg e^{-(k_1+k_2)}$, it is simplified to a first-order rate of swelling

$$\frac{Q_t}{Q_\infty} \approx 1 - e^{-k_1 t} \tag{7}$$

However, for some hydrogels, near the equimolecular composition and for the most acidic pH of soaking, another process was suspected. It was observed that an induction or delay period exists, which may be caused by a higher hydrogen bond strength. In that case, swelling was interpreted in terms of two simultaneous processes: the first one follows a first-order kinetics with a very small rate constant and the second one the overall autocatalytic process with its two rate constants. The whole swelling process was represented by the following overall equation:

$$\frac{Q_t}{Q_\infty} = \beta \frac{(k_1/k_2)(1 - e^{-(k_1+k_2)t})}{(k_1/k_2) + e^{-(k_1+k_2)t}} + (1 - \beta)(1 - e^{-k_3 t}) \tag{8}$$

in which β is a parameter which represents the fraction of each one of the two contributions to the overall process. This assumption is now supported by the MRI experiments. The first slow process could correspond to the swelling of the outer part of the gel. We have intended to separate these two processes starting from the images by integrating the first stages of the swelling process, i.e., the two zones of different intensity, for the two samples in which the swelling process is slower. For example, in Figure 5, images corresponding to different stages of swelling for 25% mol *N*-iPAAm hydrogel have been shown. One can observe that there exists an external yellow zone of equal intensity well differentiated of the center, that is the swelling front; the intensity of this part has been integrated and substrated to the total integral intensity. In Figure 5 white and

black dotted lines indicate these two regions. The deconvolution cannot be done for the whole swelling process because sometime the second process overlaps the first one. In Figure 10a,b deconvolution curves of these two simultaneous processes represented by eq 8 corresponding to 25 and 42% *N*-iPAAm contents are shown. The fitting of the experimental results has been done as follows: the integral of the intensity of the first process, the water uptake of the external part of the gel, represented in full squares, has been adjusted to a first-order kinetics (second term of eq 8), from this fitting the values of β and k_3, have been obtained, and then these values have been considered fixed in eq 8, to fit the whole integral intensity (represented as open squares), thus obtaining k_1 and k_2 rate constants.

The kinetic parameters resulting from the deconvolution for 42% *N*-iPAAm copolymer are $k_1 = 1.58 \times 10^{-6}$ min, $k_2 = 4.53 \times 10^{-3}$ min, $k_3 = 1.48 \times 10^{-3}$ min, and $\beta = 0.2575$. For 25% *N*-iPAAm $k_1 = 9 \times 10^{-5}$ min, $k_2 = 4.21 \times 10^{-3}$ min, $k_3 = 1.55 \times 10^{-3}$ min, and $\beta = 0.2345$.

In both cases the attack of the swelling front, controlled by k_3, occurs at a similar rate, and the fraction of polymer swollen by this first process is also comparable. The major difference between these two copolymers lies on the catalytic process; k_1 and k_2 are higher for 25% mol *N*-iPAAm copolymer, especially k_1, which corresponds with the faster autoacceleration swelling observed for this copolymer.

To test that the swelling in the most external part may follow a first-order kinetics, we have carried out the same experiment using a 42% mol N-iPAAm content sample, however in this case with a sample of cylindrical shape with a diameter of 0.5 and 1 cm length. The recorded images for a radial cut plane as well as the extracted one-dimensional profiles as a function of time are shown in Figure 11a,b. As we can see in this figure, the swelling front moves very slowly. By plotting the integral of the profile as a function of time, Figure 11c, it can be observed that it follows a first-order kinetics.

As we have mentioned before, the anomalous behavior of the swelling is directly related to the presence of hydrogen bond arrangements in the sample, and it disappears when the sample has not been submitted before to acid treatment. In Figure 12, the NMR images recorded for the sample of a 42% mol N-iPAAm composition, previously soaked at acidic pH (a) and the images recorded for a sample with identical composition, which was not soaked at pH 2, are shown for comparative purposes. It can be appreciated that when the sample is free of hydrogen bond arrangements, the swelling is very fast and follows a first-order kinetics.

Patterns exhibiting a sigmoidal swelling with accelerating aqueous uptaking rates during swellings, as we have made mention before, have been also found in different systems,[18−30] and although their authors do not make mention it can be observed in other systems such as i.e. in comblike polymers poly[(methacrylic acid)-*g*-(ethylene glycol)] and poly[(methacrylic)-*g*-(propylene glycol)].[49] From all these authors, only Siegel[18,19] has given a mechanistic approach to the interpenetration of the sigmoidal swelling observed for a hydrophobic weak base polyelectrolyte copolymer of methyl methacrylate (MAA) and *N*,*N*-dimethylamino methacrylate (DMA). Siegel[19] suggested that the transport of protons from the outer solution to uncharged amines at the swelling front is limiting the swelling, since a combination of solvent and ions must be present

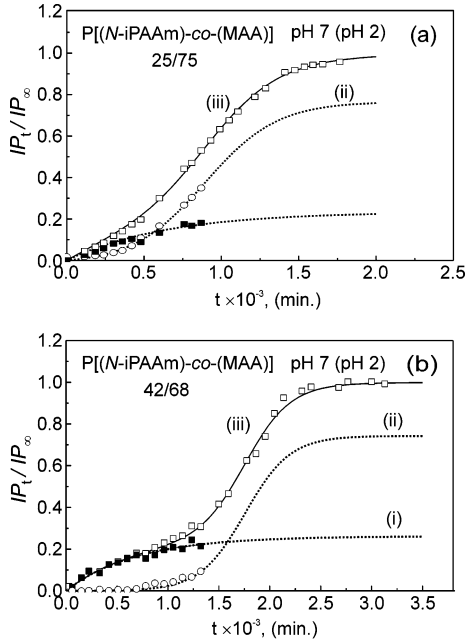

Figure 10. Deconvolution in a first order (i) and an autocatalytic (ii) processes from the dynamic swelling isotherm, of magnetic resonance imaging (MRI) data (iii) according to eq 8, as a function of the normalized integral of the spin density profiles IP_t/IP_∞ vs time t of two samples of P[(N-iPAAm)-*co*-(MAA)] with 25 (a) 42 (b) % mol N-iPAAm contents, crosslinked with 0.5 wt % of TEGDMA. These two processes have been separated directly from experimental data starting from the images by integrating the first stages of the swelling process, i.e., the two zones of different intensity, for the two samples in which the swelling process is slower. They are represented in the figures by (■) full squares and (○) open circles, respectively.

to initiate a glass to rubber transition, in the early stages of swelling; a swelling front separates a swollen outer region from a glassy core owing to case II transport mechanisms. The front proceeds toward the glassy interior as the polymer absorbs water. In this process, the glassy core largely constrains the swelling in the direction normal to the front. When the fronts meet at the midpoint of the polymer starts to swell largely unidirectional because the swelling constraint disappears. Therefore, the swelling of the gels is suddenly accelerated.[22] The work reported by Siegel[19,18,22] is quite interesting and completed, especially about the influence of the medium characteristics on the swelling behavior, as the buffer identity, buffer concentration, pH, etc. However, by means of the imaging experiments, information about when and how acceleration occurs can be provided. Thus, we have observed that acceleration takes place before the swelling front reaches the middle point in the sample. This is contrary to the argument suggested by Siegel;[22] the degree of swelling of the swelling front is not really constrained by the glassy core. In fact, according to our observations, the swelling characteristics for these samples can be summarized as follows: in a first stage, the most external part of the specimen starts to swell; its swelling is slow, but it takes place completely all over the specimen, thus appearing as a swelling front. The advance of the front is governed in its neighborhoods by the disruption of the hydrophobic hydrogen bond arrangements. Since the external zone reach high swelling values, the volume difference of this part compared with the adjacent center makes the external part to refold forming like a scallop around its center, at the same time that a curious relief

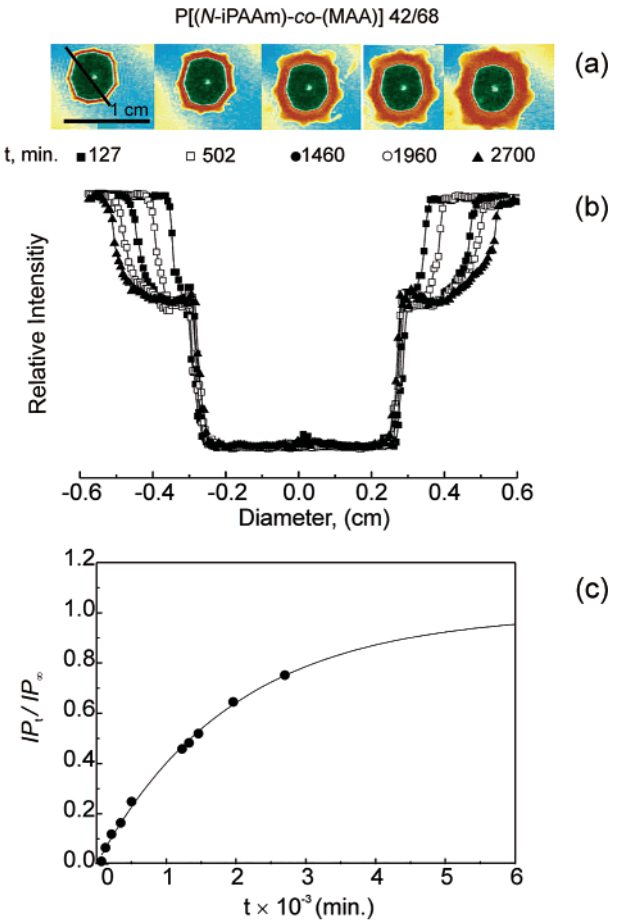

Figure 11. (a) Primary magnetic resonance imaging (MRI) data from a cylindrical specimen of the dynamic swelling isotherms in water at pH 7 and 25 °C of P[(N-iPAAm)-*co*-(MAA)] 42/58 cross-linked with 0.5% of TEGDMA and previously soaked at pH 2. (b) A series of one-dimensional signal intensity profiles obtained using the spin-echo sequence which was applied after increasing time of swelling as it is indicated and taken perpendicular to the cylinder axis. (c) Dynamic swelling isotherms from proton MRI images as a function of IP_t/IP_∞, the normalized integral of the intensity corresponding to the profiles plotted in (a), vs time t. The data fits to a first-order kinetics with a rate constant of 5.1×10^{-4} min^{-1}.

on both disk surfaces appears, which is clearly seen in the photographs. In a second stage, depending on the gel composition besides, the swelling is accelerated because some buffer is able to go inside the core, thus promoting a rapid and cooperative hydrogen bond disruption. It is interesting to note that at this stage the sample core becomes white and opaque. Later on, the sample starts to growth more homogeneously, getting an almost uniform circular shape and finally having the appearance of a disk. The shape of the swelling curve and the swelling rate are clearly a function of the sample composition.

Siegel[19,22] suggested that the buffer is a carrier of ions, hence the crucial importance of the kind of buffer. Similarly he observed that the pH has a strong influence on the swelling as we have also pointed out. However, the appearance of swelling sigmoidal curves cannot be justified solely by the transport of ions in the case of an ionizable polymer, since then this type of phenomena would appear as well in the P(MAA) homopolymer. But it cannot be attributed, as an isolated form, to the rupture of hydrogen bonds, since they are also presented in the P(MAA) homopolymer. It is our believe that this

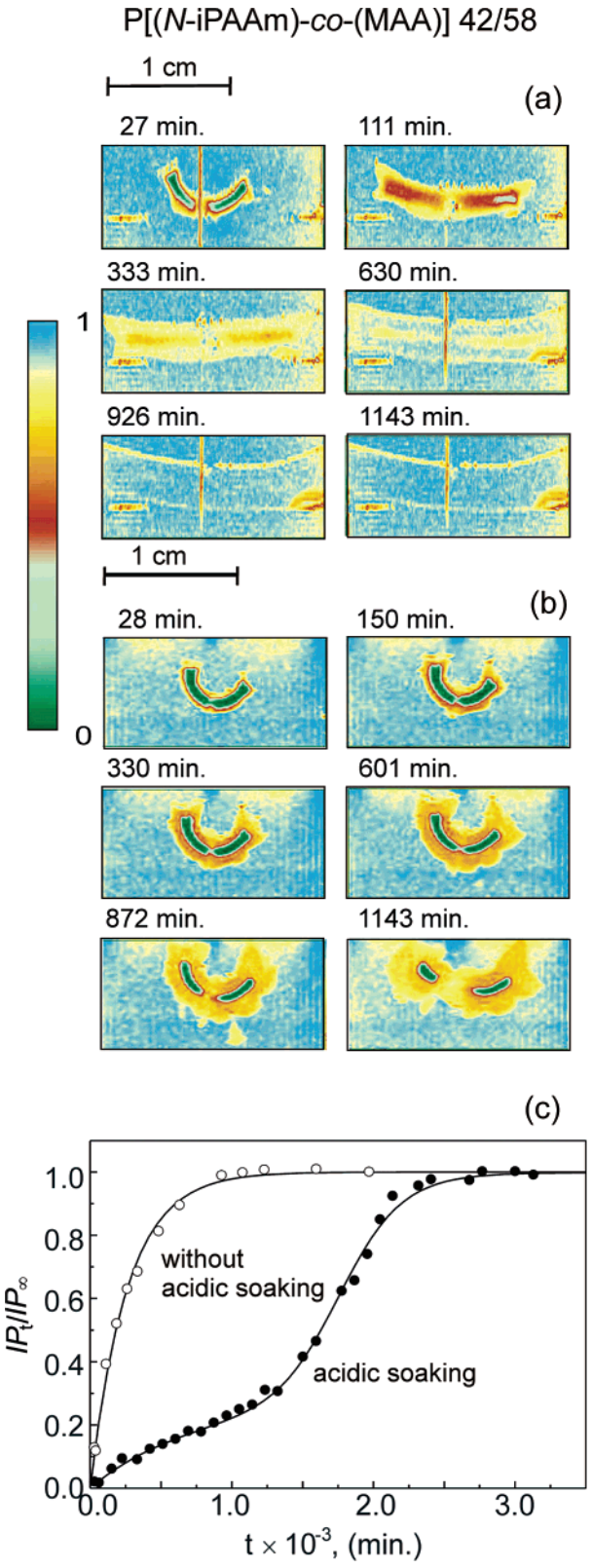

Figure 12. (a) Proton MRI images corresponding to the dynamic swelling isotherms of P[(N-iPAAm)-*co*-(MAA)] 42/58 cross-linked with 0.5 wt % of TEGDMA in water at pH 7 and 25 °C: (a) sample without any previously soaking treatment and (b) sample previously soaked at pH 2. (c) Swelling curves as a function of the normalized integral of the one-dimensional signal intensity profiles IP_t/IP_∞ vs time t, measured along the concave axis of the samples.

behavior obeys to the fact that in these cases the hydrogen bonds are more inaccessible to water molecules since they are stabilized by hydrophobic interac-

tions. The key of this behavior lies in the influence of the composition. Thus, copolymers with a composition of almost the equimolecularity show a slower kinetics and a sigmoidal trend much more remarkable. This fact could be indicative that the origin of this behavior is an effective interaction between both structural units. This interaction might be promoted by soaking previously of the hydrogels at low pH.

Conclusions

MRI has been used successfully to monitor water uptake into P[(N-iPAAm)-*co*-(MAA)] copolymers. The main purpose of the present MRI study was the temporally and spatially resolved analysis of the penetration and distribution of water as a function of the copolymer composition. MRI proved to be a valuable tool for precisely and nondestructively analyzing the behavior of the same specimen of P[(N-iPAAm)-*co*-(MAA)] copolymers during water uptaking.

The experimental results presented in this paper clearly demonstrate the differences in the swelling behavior as a function of hydrogel composition and pH of previous soaking.

Because of the monitorization of the state of water in the inner part of the gel which has been furnished by the NMR imaging experiments, we can say that the experimental sigmoidal swelling curves might be explained by the existence of two swelling processes. The first process, which corresponds to the swelling of the external zone of the gel, produces a swelling front that progresses slowly to the inner zone. Then, the second process is autoacceleration, which could be justified very precisely by the cooperative disruption of the hydrogen bonds and the weakness of the hydrophobic interactions in the inner part of the gel.

The change of the swelling mechanism with pH and composition may provide very valuable information for the application of P[(N-iPPAm)-*co*-(MAA)] copolymers matrices in the preparation of controlled release drugs.

Acknowledgment. The authors gratefully acknowledge the financial assistance of the Comisión Interministerial de Ciencia y Tecnología of the Subdirección General de Proyectos of the Ministerio de Ciencia y Tecnología (MAT2002-04042-002-02). Isabel Quijada-Garrido acknowledges the award of a Ramón y Cajal Contract of the Ministerio de Ciencia y Tecnología. Alberto Prior-Cabanillas is also thankful for a Grant-in-Aid sponsored by the Ministerio de Ciencia y Tecnología.

References and Notes

(1) Brazel, C. S.; Peppas, N. A. *Macromolecules* **1995**, *28*, 8016−8020.
(2) Brazel, C. S.; Peppas, N. A. *J. Controlled Release* **1996**, *39*, 57−64.
(3) Huglin, M. B.; Liu, Y.; Velada, J. L. *Polymer* **1997**, *38*, 5785−5791.
(4) Vakkalanka, S. K.; Brazel, C. S.; Peppas, N. A. *J. Biomater. Sci., Polym. Ed.* **1996**, *8*, 119−129.
(5) Yang, H. H.; Zhu, Q. Z.; Chen, S.; Li, D. H.; Chen, X. L.; Ding, M. T.; Xu, J. G. *Anal. Biochem.* **2001**, *296*, 167−1173.
(6) Kono, K.; Okabe, H.; Morimoto, K.; Takagishi, T. *J. Appl. Polym. Sci.* **2000**, *77*, 2703−2710.
(7) Xue, W.; Champ, S.; Huglin, M. B. *Polymer* **2000**, *41*, 7575−7581.
(8) Díez-Peña, E.; Quijada-Garrido, I.; Barrales-Rienda, J. M.; Wilhelm, M.; Spiess, H. W. *Macromol. Chem. Phys.* **2002**, *203*, 491−502.
(9) Díez-Peña, E.; Quijada-Garrido, I.; Frutos, P.; Barrales-Rienda, J. M. *Macromolecules* **2002**, *35*, 2667−2675.
(10) Díez-Peña, E.; Quijada-Garrido, I.; Barrales-Rienda, J. M. *Polymer* **2002**, *43*, 4341−4348.
(11) Díez-Peña, E.; Quijada-Garrido, I.; Barrales-Rienda, J. M. *Macromolecules* **2002**, *35*, 8882−8888.
(12) Díez-Peña, E.; Frutos, P.; Frutos, G.; Quijada-Garrido, I.; Barrales-Rienda, J. M. *AAPS Pharm. Sci. Technol.* **2004**, *5*, paper 33.
(13) Sousa, R. G.; Prior-Cabanillas, A.; Quijada-Garrido, I.; Barrales-Rienda, J. M. *J. Controlled Release* **2005**, *102*, 595−606.
(14) Zhang, K.; Wu X. Y. *J. Controlled Release* **2002**, *80*, 169−178.
(15) Heskins, M.; Guillet, J. E. *J. Macromol. Sci. Chem. A2* **1968**, *8*, 1441−1455.
(16) Shild, H. G. *Prog. Polym. Sci.* **1992**, *17*, 163−249.
(17) Díez-Peña, E.; Quijada-Garrido, I.; Frutos, P.; Barrales-Rienda, J. M.; Schnell, I.; Spiess, H. W. *Macromol. Chem. Phys.* **2004**, *205*, 438−447.
(18) Firestone, B. A.; Siegel, R. A. *J. Appl. Polym. Sci.* **1991**, *43*, 901−904.
(19) Siegel, R. A. *Adv. Polym. Sci.* **1993**, *109*, 233−267.
(20) Yoshida, R.; Okuyama, Y.; Sakai, K.; Okano, T.; Sakurai, Y. *J. Membr. Sci.* **1994**, *89*, 267−277.
(21) Okuyama, Y.; Yoshida, R.; Sakai, K.; Okano, T.; Sakurai, Y. *J. Biomater. Sci., Polym. Ed.* **1993**, *4*, 545−556.
(22) Siegel, R. A. In Kost, J., Ed.; *Pulsed and Self-Regulated Drug Delivery*; CRC Press: Boca Raton, FL, 1990; pp 129−157.
(23) Falamarzian, M.; Firestone, B. A.; Moxley, B. C. *J. Controlled Release* **1988**, *8*, 179−182.
(24) Falamarzian, M.; Varshosaz, J. *J. Drug Dev. Ind. Pharm.* **1998**, *24*, 667−668.
(25) Kim, B.; La Flamme, K.; Peppas, N. A. *J. Appl. Polym. Sci.* **2003**, *89*, 1606−1613.
(26) Kim, B.; Peppas, N. A. *Biomed. Microdevices* **2003**, *5*, 333−341.
(27) Brazel, C. S.; Peppas, N. A. *Polymer* **1999**, *40*, 3383−3398.
(28) Milroy, G. E.; Cameron, R. E.; Mantle, M. D.; Gladden, L. F.; Huatan, H. *J. Mater. Sci., Mater. Med.* **2003**, *14*, 465−473.
(29) Wang, C.; Stewart, R. J.; Kopeèek, J. *Nature (London)* **1999**, *397*, 417−420.
(30) Traitel, T.; Kost, J.; Lapidot, S. A. *Biotechnol. Bioeng.* **2003**, *84*, 20−28.
(31) Díez-Peña, E.; Quijada-Garrido, I.; Frutos, P.; Barrales-Rienda, J. M. *Polym. Int.* **2003**, *52*, 956−965.
(32) Prior-Cabanillas, A.; Quijada-Garrido, I.; Frutos, G.; Barrales-Rienda, J. M. *Polymer* **2005**, *46*, 685−693.
(33) Melia, C. D.; Rajabi-Siahboomi, A. R.; Bowtell, R. W. *Pharm. Sci. Technol. Today* **1998**, *1*, 32−39.
(34) Snaar, J. E. M.; Bowtell, R. W.; Melia, C. D.; Morgan, S.; Narasimhan, B.; Peppas, N. A. *Magn. Reson. Imaging* **1998**, *16*, 691−694.
(35) Ercken, M.; Adriaensens, P.; Reggers, G.; Carleer, R.; Vanderzande, D.; Gelan, J. *Macromolecules* **1996**, *29*, 5671−5677.
(36) Kuhn, W. *Macromolecules* **1998**, *31*, 3886−3894.
(37) Knörgen, M.; Arndt, K.-F.; Richter, S.; Kuckling, D.; Schneider, H. *J. Mol. Struct.* **2000**, *554*, 69−79.
(38) Mansfield, P.; Bowtell, R. W.; Blackband, S. *J. Magn. Reson.* **1992**, *99*, 507−524.
(39) Bowtell, R.; Sharp, J. C.; Peters, A.; Mansfield, P.; Rajabi-Siahboomi, A. R.; Davies, M. C.; Melia, C. D. *Magn. Reson. Imaging* **1994**, *12*, 361−364.
(40) Rajabi-Siahboomi, A. R.; Bowtell, R.; Mansfield, P.; Henderson, A.; Davies, M. C.; Melia, C. D. *J. Controlled Release* **1994**, *21*, 121−134.
(41) Snaar, J. E. M.; Bowtell, R.; Melia, C. D.; Morgan, S.; Narasimhan, B. *Magn. Reson. Imaging* **1998**, *16*, 691−694.
(42) Mansfield, P.; Morris, M. G. *NMR Imaging in Biomedicine*; Adv. Magn. Reson. Suppl. 2; Academic Press: New York, 1982.
(43) Blümich, B. *NMR Imaging of Materials;* Clarendon Press: Oxford, 2000.
(44) Crank, J.; Park, G. S. *Diffusion in Polymers*; Academic Press: New York, 1968.
(45) Marom, G. In *Polymer Permeability*; Comyn, J., Ed.; Elsevier. New York, 1975; p 341.
(46) Alfrey, T., Jr.; Gurnee, E. F.; Lloyd, W. G. *J. Polym. Sci., Part C* **1966**, *12*, 249−261.
(47) Franson, N. M.; Peppas, N. A. *J. Appl. Polym. Sci.* **1983**, *28*, 1299−1310.
(48) Berens, A. R.; Hopfenberg, H. B. *Polymer* **1978**, *19*, 489−496.
(49) Prior Cabanillas, A.; Quijada-Garrido, I.; Barrales-Rienda, J. M., to be published.

MA0509513